Translational Oncology
www.transonc.com

Volume 5 Number 6 December 2012 pp. 408–414 408

Microscopic Delineation of Medulloblastoma Margins in a Transgenic Mouse Model Using a Topically Applied VEGFR-1 Probe[1]

Danni Wang*, Ye Chen*, Steven Y. Leigh*, Henry Haeberle†, Christopher H. Contag† and Jonathan T. C. Liu*

*Department of Biomedical Engineering, State University of New York (SUNY) at Stony Brook, Stony Brook, NY; †Clark Center, Stanford University School of Medicine, Stanford, CA

Abstract

The unambiguous demarcation of tumor margins is critical at the final stages in the surgical treatment of brain tumors because patient outcomes have been shown to correlate with the extent of resection. Real-time high-resolution imaging with the aid of a tumor-targeting fluorescent contrast agent has the potential to enable intraoperative differentiation of tumor *versus* normal tissues with accuracy approaching the current gold standard of histopathology. In this study, a monoclonal antibody targeting the vascular endothelial growth factor receptor 1 (VEGFR-1) was conjugated to fluorophores and evaluated as a tumor contrast agent in a transgenic mouse model of medulloblastoma. The probe was administered topically, and its efficacy as an imaging agent was evaluated *in vitro* using flow cytometry, as well as *ex vivo* on fixed and fresh tissues through immunohistochemistry and dual-axis confocal microscopy, respectively. Results show a preferential binding to tumor *versus* normal tissue, suggesting that a topically applied VEGFR-1 probe can potentially be used with real-time intraoperative optical sectioning microscopy to guide brain tumor resections.

Translational Oncology (2012) 5, 408–414

Introduction

Medulloblastoma is the most common malignant pediatric brain tumor. Despite the availability and advancement of medical technologies, patient prognoses remain poor [1,2]. Bulk tumor resection remains the first line of treatment, where it has been shown that the completeness of tumor resection correlates strongly with the survival of patients [1–3]. The goal of neurosurgeons is to maximize the removal of tumor while minimizing the removal of normal tissues. The current gold standard for assessing malignancy is histopathology of biopsied tissue samples. However, this is rarely performed at the tumor margins during resection because of the time required for frozen sections to be prepared and interpreted by a pathologist. Furthermore, histopathology is expensive and requires the removal of brain tissue regardless of the state of the tissue. Therefore, there is a need for a noninvasive method to rapidly and accurately visualize residual malignancy to assist surgeons during the tumor resection process.

In previous work, we developed a handheld dual-axis confocal (DAC) microscope for intraoperative optical biopsy at the tumor margins [4]. An optical sectioning microscope with cellular resolution has the potential to provide highly accurate confirmation of tissue status with the possibility of optimizing and complementing low-resolution wide-field imaging approaches such as fluorescence image–guided surgery [5–7]. Reports from early preclinical and clinical studies suggest that intraoperative confocal microscopy can play a valuable role in guiding tumor resection, especially in certain tumor types that do not image well with wide-field techniques [8–11].

In this study, we are developing a contrast agent to be used in conjunction with point-of-care confocal microscopes and other forms of fluorescence imaging. The vascular endothelial growth factor receptor 1 (VEGFR-1) and other tyrosine kinase receptors have been shown to be overexpressed on the surface of human medulloblastoma

Address all correspondence to: Jonathan T. C. Liu, PhD, Bioengineering G15, Stony Brook University, Stony Brook, NY 11794-5281. E-mail: jonathan.liu@stonybrook.edu
[1]The authors acknowledge funding support from the National Institute of Biomedical Imaging and Bioengineering, National Institutes of Health (NIH) (K99/R00 EB008557; J.T.C.L.), the Office of the Vice President for Research at Stony Brook University (J.T.C.L.), National Cancer Institute, NIH (U54 CA 136465; C.H.C.), and the Stanford Center for Children's Brain Tumors (J.T.C.L. and C.H.C.).
Received 21 August 2012; Revised 21 August 2012; Accepted 13 September 2012

DOI 10.1593/tlo.12277

cell lines as well as on tumor cells in excised human medulloblastoma tissues [12], suggesting that VEGFR-1 plays a role in the development of medulloblastoma and could be a molecular target for therapeutic and imaging agents. To explore the feasibility of a VEGFR-1 imaging agent, we first demonstrated that VEGFR-1 is overexpressed in a transgenic mouse model of medulloblastoma and developed a fluorescent VEGFR-1 probe that could be topically applied on fresh tissues to provide molecular image contrast in this predictive animal model.

Materials and Methods

Transgenic Mouse Model

The *ptc*$^{+/-}$*p53*$^{-/-}$*Math1-GFP* medulloblastoma mouse model was developed previously [13,14]. These mice, which are heterozygous knockouts for *ptc* and homozygous knockouts for *p53*, develop medulloblastoma with 95% penetrance at 3 to 5 weeks of age. The tumor cells in these mice express green fluorescent protein (GFP) as driven by a *Math1* promoter, a developmental gene that is overexpressed in medulloblastoma.

Multiwavelength DAC Microscope

A custom multiwavelength DAC microscope was developed previously [15,16]. The DAC architecture allows for relatively deep optical sectioning within tissues, as demonstrated through diffraction theory modeling [17], Monte Carlo scattering simulations, tissue-phantom measurements [15], and imaging studies [15,17]. All imaging experiments of fresh thick tissues in this study were performed using the DAC microscope, which acquires serial vertical image sections across a three-dimensional volume of tissue with a maximum field of view of 600 × 800 μm and a depth of 500 μm (maximum depth varies with tissue type). The spatial resolution of the microscope is approximately 2 μm in the lateral directions and 3 μm in the vertical direction (depending on wavelength and imaging depth). Image sections are acquired at 2 frames/second with a 1-μm step size between serial vertical sections. Laser sources at 488, 660, and 785 nm were used for imaging fluorescence from GFP, Alexa Fluor 647 (AF647), and Licor IRDye 800CW, respectively. In this study, the microscope was used for two-channel imaging at 488 and 660 nm or at 660 and 785 nm.

Probe Conjugation

Monoclonal VEGFR-1 antibodies (Abcam, Cambridge, MA; ab51872) were conjugated with AF647 dye and purified using a labeling kit (Invitrogen, Grand Island, NY; A-20186). The labeling efficiency and yield were verified by spectrophotometry. Typical post-purification antibody yields were more than 80% with a labeling ratio of approximately five dye molecules per antibody, within the manufacturer's suggested range of three to seven dye molecules per antibody. Isotype control antibodies (Rat IgG2a) were purchased pre-conjugated to AF647 (eBioscience, San Diego, CA; 51-4321-82) with an average labeling ratio of three to seven dye molecules per antibody.

Primary Cell Culture

Primary medulloblastoma cells were isolated from the cerebellum of transgenic mice based on a protocol described previously [18]. In brief, the cerebellar tissue was coarsely minced with a sterile scalpel and digested using papain (2 mg/ml; Sigma-Aldrich, St Louis, MO) at 37°C for an hour. The digested tissue was triturated and passed through a 40-μm cell strainer to yield the final single-cell suspension. The cells were either immediately used for flow cytometric analysis or maintained for future use as neurosphere suspensions in Neurobasal/B27-without-Vitamin-A medium with non-essential amino acids, 1 mM L-glutamine, 1% penicillin/streptomycin, and 1% sodium pyruvate and supplemented with epidermal growth factor and β-fibroblast growth factor. Gross confirmation of the success of primary tumor cell isolation was done visually using a blue light source and GFP viewing filter (Nightsea, Inc, Bedford, MA).

Flow Cytometry

Isolated primary cerebellar cell samples were stained using AF647-conjugated VEGFR-1 monoclonal antibody (mAb) or an AF647-conjugated isotype control mAb. Samples were incubated for 15 minutes at room temperature and rinsed once using phosphate-buffered saline (PBS)/FBS buffer before flow cytometric analysis was performed with a FACSCalibur flow cytometer (BD Biosciences, San Jose, CA). Analyses were performed using Flowjo software to confirm the co-localization of GFP and AF647 (VEGFR-1) on the primary cells.

Immunohistochemistry

Cerebellar tissues obtained from the transgenic medulloblastoma mice were fixed in ice-cold 4% paraformaldehyde for 1 hour and cryoprotected through dehydration using a 30% sucrose solution in PBS overnight. The preserved tissues were frozen in optical cutting temperature compound, sectioned with a cryotome at a thickness of 20 μm (at −18°C), and mounted onto slides. Each slide contained three consecutive brain sections, which were stained with AF647-conjugated VEGFR-1 antibodies, matching AF647-conjugated isotype antibody, and PBS, respectively. Staining durations ranged from 5 to 15 minutes and were limited to these short durations to mimic the conditions that will eventually be required for *in vivo* surgical use. Stained slides were rinsed for 5 minutes in PBS and then sealed with an aqueous mounting media and a coverslip. The slides were imaged with a commercial confocal microscope (Leica TCS SP5 II) to visualize the co-localization of GFP-expressing tumors and the AF647 dye (VEGFR-1 mAb) at the tumor margins. Image panels were analyzed using ImageJ [19]. A total of $n = 17$ different tumor margin locations from different animals were imaged. For each image of a tumor margin, five regions of interest (ROIs) were selected from within the tumor region as well as within the normal region (10 ROIs in total). Images obtained from the GFP channel were used to identify tumor *versus* normal regions. An average signal intensity was determined for each tumor and normal ROI, and these signals were again averaged across the five tumor ROIs and the five normal ROIs to determine a tumor-to-normal intensity ratio for each image.

DAC Microscopy of Fresh Thick Tissues

Freshly excised thick tumor margins, identified macroscopically using a blue light source and GFP viewing filter, were immediately stained with AF647-conjugated VEGFR-1 mAb or AF647-conjugated isotype control. Probe application on *ex vivo* tissue samples was performed topically by soaking samples in a 0.1 mg/ml probe solution prepared with 5% DMSO in PBS for 10 minutes, followed by rinse removal of unbound probe by soaking the stained tissue three times for 1 minute each in PBS. Numerous researchers have used up to 10% and 20% DMSO to enhance the delivery of contrast agents

[20–22] for shallow subsurface imaging. Likewise, in this study, the addition of 5% DMSO was used to enhance the permeation of our antibody probes during topical delivery. Samples were imaged with a custom multiwavelength DAC microscope, as described previously. Serial vertical image sections were obtained, and image stacks were volume-rendered using AMIRA software. Images of horizontal sections, from depths ranging from 25 to 75 μm, were exported and analyzed using ImageJ as was performed for images from physically sectioned slides. Average tumor-to-normal pixel intensity ratios were calculated from n = 20 samples of thick brain tissues from different animals.

Quantitative Ratiometric Imaging

To confirm and quantify the binding specificity of the VEGFR-1 probe during thick tissue microscopy, we used a previously developed ratiometric imaging strategy [16]. This method involves the simultaneous imaging of a targeted (VEGFR-1 mAb) and an untargeted (isotype control) probe. Freshly excised tumor-margin specimens were stained with an equimolar mixture of Licor 800CW-conjugated VEGFR-1 mAb (785-nm excitation) and AF647-conjugated isotype mAb (660-nm excitation), incubated at room temperature for 10 minutes, and rinsed with PBS (three times). Before the imaging of tissue specimens, system calibration was done by imaging an equimolar mixture of the probe and isotype mAb solution at the exact laser and detector gain settings used for subsequent tissue imaging. The ratio of the average intensity from each channel was used as a calibration factor for ratiometric quantification of specific *versus* nonspecific binding of the imaging probes in tissue, as detailed previously [16]. Images were processed and calibrated in MATLAB (MathWorks, Natick, MA) and ImageJ.

Statistical Analysis

Results summarized in Table 1 are presented as mean ± 1 standard deviation. The normality of all data series was established using the Shapiro-Wilk test. Median ratios are also presented in the table to indicate that outliers, if present, do not affect the validity of our assessments. Results were analyzed using an independent sample t test as well as Wilcoxon test to determine statistical difference between the tumor-to-normal ratios of isotype and probe-stained tissues. In both cases, the significance level was set as $\alpha = 0.01$. All statistical analyses were performed using the Analyse-it add-in to Microsoft Excel.

Results

Flow Cytometry of Primary Cultured Cells

Preliminary flow cytometry of primary cultured cerebellar cells revealed that a subpopulation of GFP-expressing medulloblastoma cells (~5%) exhibited a significant elevated expression (10-fold to 100-fold) of VEGFR-1. These results provided motivation to pursue immunohistochemistry (IHC) analysis and, later, DAC microscopy of fresh thick tissues.

Table 1. Summary of Imaging Analysis.

Groups	n	Staining	Median T/N Ratio	Average T/N Ratio
Fixed sections	17	VEGFR-1	1.77	1.84 ± 0.26
	17	Isotype	1.32	1.36 ± 0.25
Fresh thick tissue	20	VEGFR-1	3.25	3.46 ± 1.18
	20	Isotype	1.88	1.81 ± 0.65

The sample size n is defined as the number of frozen sections for IHC and the number of tumor-margin specimens obtained from different animals for fresh tissue imaging.

Immunohistochemistry

Fixed frozen sections of mouse medulloblastoma tissue show clear preferential binding of VEGFR-1 mAb to tumor in comparison to normal tissue, while the isotype control shows relatively uniform nonspecific binding to both tumor and normal regions (Figure 1). Average tumor-to-normal intensity ratios are calculated for n = 17 samples by taking the ratio of the average intensity from five tumor and five normal ROIs within each tissue section. The average tumor-to-normal intensity ratio is 1.84 ± 0.26 for VEGFR-1 probe–stained slides and 1.36 ± 0.25 for the isotype-stained counterparts. The box-and-whisker plot in Figure 1*G* shows the results from n = 17 different tumor margin locations from different animals. Each box plot presents the full-range distribution of the data set indicating the 25th, 50th, and 75th percentiles along with the maximum and minimum values. The statistical difference between the two groups was found to be significant at $P < .01$. The tumor-to-normal intensity ratios for the representative images shown in Figure 1, *B* and *E*, are 1.72 and 1.08, respectively.

DAC Microscopy of Fresh Thick Tissues

Freshly excised mouse medulloblastoma margins stained with AF647-conjugated VEGFR-1 mAb show clear co-localization with GFP-positive tumor tissues, while the isotype control does not (Figure 2, *A* and *B*). Average tumor-to-normal intensity ratios are calculated for n = 20 fresh thick tissue samples by taking the ratio of the average intensity from five tumor and five normal ROIs within each tissue at a single optical section depth. The average tumor-to-normal intensity ratio is 3.46 ± 1.18 for VEGFR-1–stained tissues and 1.81 ± 0.65 for isotype-stained thick tissue specimens. The box-and-whisker plot in Figure 2*C* shows the results from n = 20 different tumor margin locations from different animals. Each box plot presents the full range distribution of the data set indicating the 25th, 50th, and 75th percentiles along with the maximum and minimum values. The statistical difference between the two groups was found to be significant at $P < .01$. The tumor-to-normal intensity ratios for the representative data shown in Figure 2, *A* and *B*, are 3.78 and 1.76, respectively.

Table 1 summarizes the results from IHC analysis of fixed frozen sections as well as DAC microscopy (optical sectioning) of fresh thick tissues.

Quantitative Ratiometric Imaging

The ratiometric imaging method allows for the quantification of molecularly specific *versus* nonspecific probe accumulation in a highly controlled fashion. The motivation for this technique, in the context of molecular microscopy with exogenous probes, will be discussed in the following section. In our ratiometric imaging strategy, a specific and a nonspecific probe are simultaneously applied onto tissue samples and simultaneously imaged with complete spatial and temporal co-registration [16]. The calibrated ratiometric image shown in Figure 3*C* provides enhanced contrast between tumor (bottom left of image) and normal tissue (upper right of image) and also provides a quantitative display of the concentration of VEGFR-1–specific probe (C_{specific}) *versus* the concentration of nonspecific probe ($C_{\text{nonspecific}}$). Line-profile analysis is done along the lines shown in Figure 3, *A* to *C*, to further

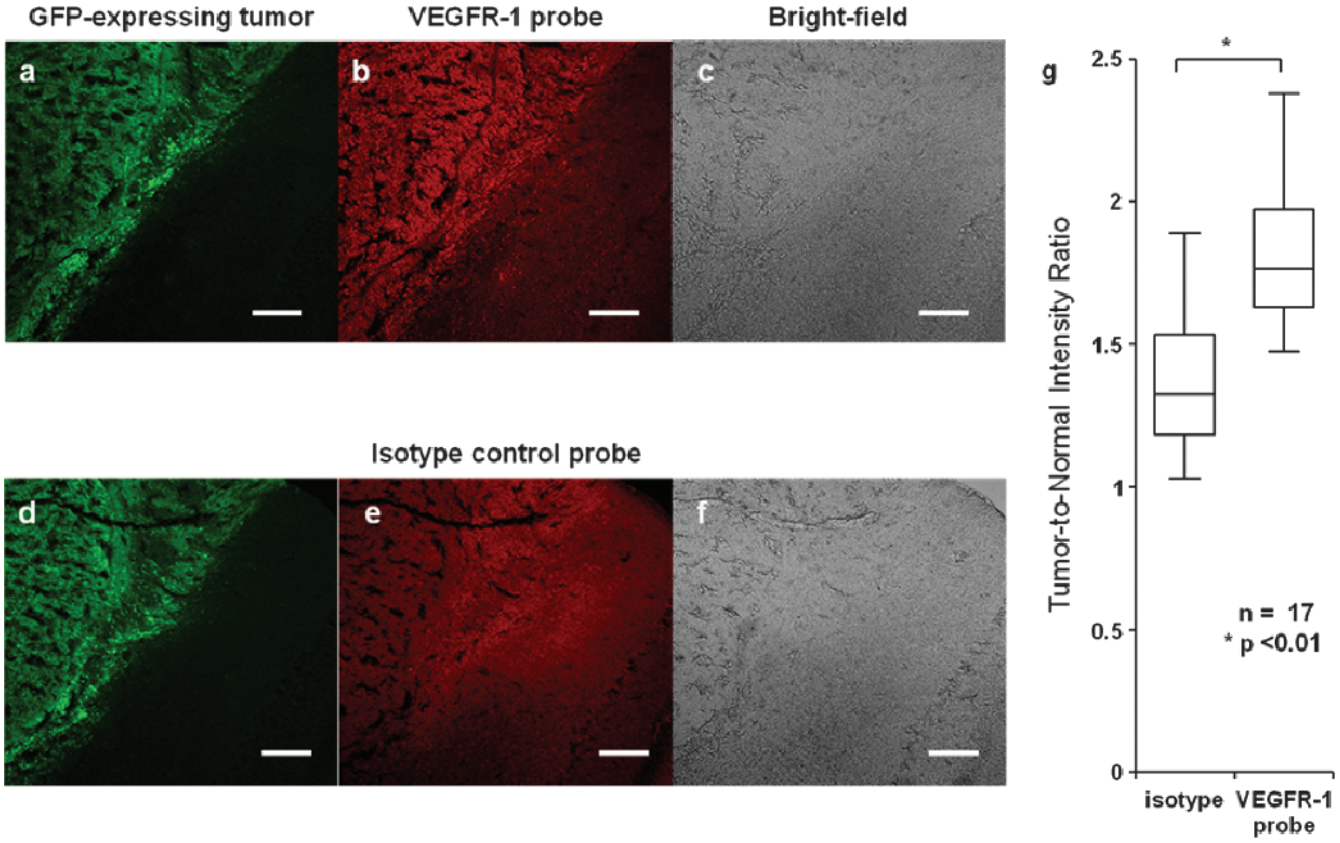

Figure 1. Physically sectioned tumor margins. Green channel: GFP-expressing tumor (A, D). Red channel: tissue stained with AF647-conjugated VEGFR-1 mAb (B) and AF647-conjugated isotype control (E). Bright-field images of the medulloblastoma tissue sections (C, F). Tumor-to-normal intensity ratio for tissue sections stained with the isotype control probe and the VEGFR-1 probe (G). Scale bar indicates 100 μm.

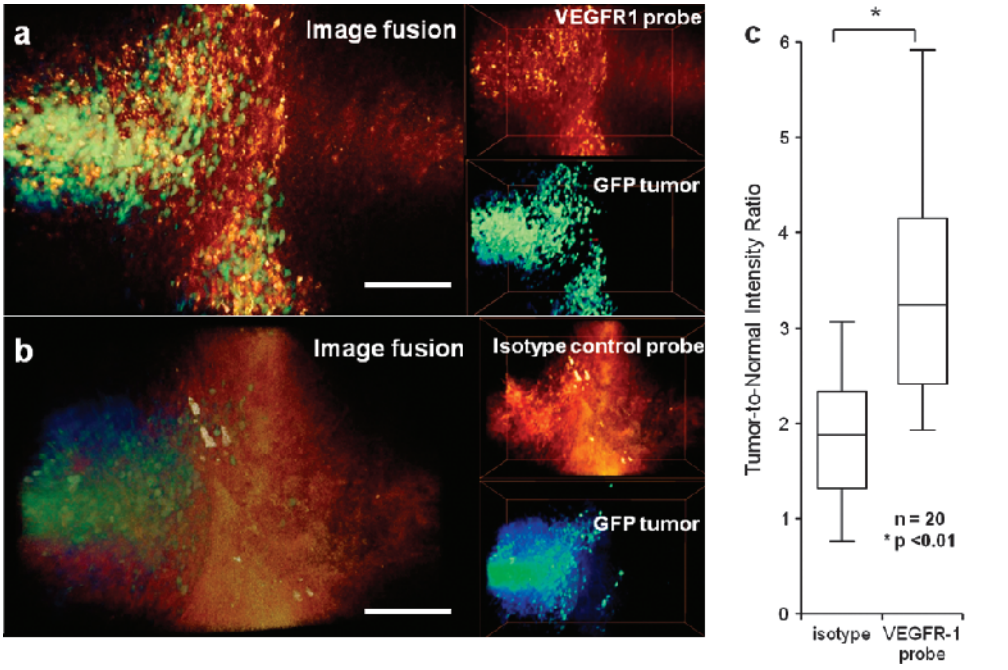

Figure 2. DAC microscope images of freshly excised thick tumor-margin specimens of medulloblastoma. (A) Volume rendering of GFP-expressing medulloblastoma and VEGFR-1 probe (overlay on the left and individual image channels on the right). (B) Volume rendering of GFP-expressing medulloblastoma and isotype control probe (overlay on the left and individual image channels on the right). (C) Tumor-to-normal intensity ratio for tissues stained with the isotype control probe and the VEGFR-1 probe. Scale bar indicates 100 μm.

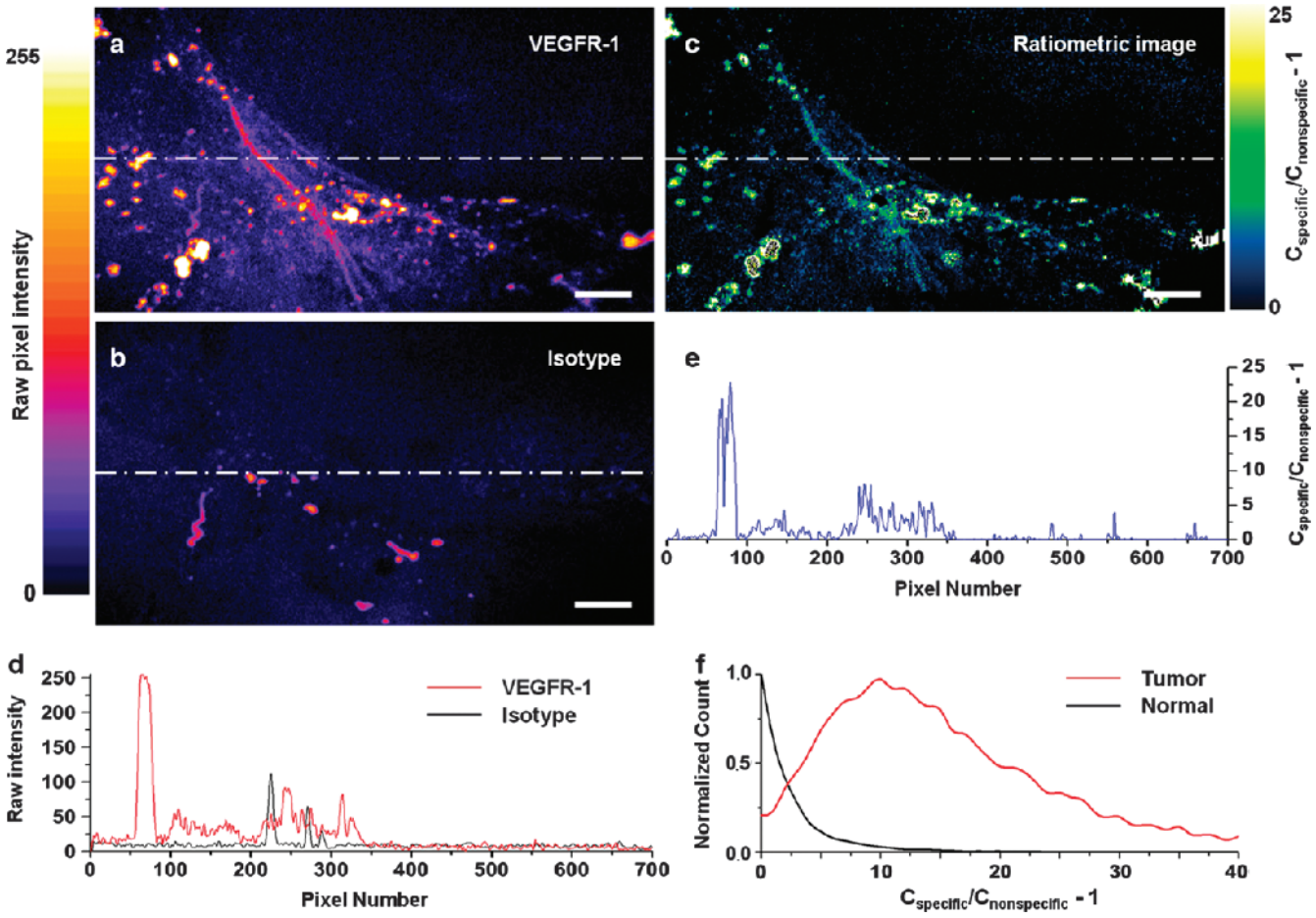

Figure 3. Quantitative ratiometric imaging of a tumor-margin specimen. Raw fluorescence image of a tumor margin stained with (A) the VEGFR-1 probe (785-nm fluorescence excitation) and (B) the isotype control probe (660-nm fluorescence excitation). (C) Calibrated ratiometric image that quantifies the specific *versus* nonspecific probe concentrations. The color map indicates the level of specific binding ($C_{specific}$) *versus* nonspecific probe accumulation ($C_{nonspecific}$). (D) Line-profile analysis of raw image intensities. (E) Line-profile analysis of the calibrated ratiometric image. (F) Normalized histogram of specific *versus* nonspecific binding to tumor and normal tissues. Scale bar indicates 50 μm.

demonstrate the ratiometric calibrated imaging technique (Figure 3, *D* and *E*). The histogram in Figure 3*F* displays the normalized distribution of specific *versus* nonspecific probe concentrations ($C_{specific}/C_{nonspecific} - 1$) for ROIs within the tumor and normal regions of the optical section shown in Figure 3*C*.

Discussion

Flow cytometry of primary cultured cells from our mouse medulloblastoma model was first used to screen for VEGFR-1 overexpression by tumor cells. The results revealed high overexpression of VEGFR-1 (10-fold to 100-fold) in a subpopulation of cells and led to the pursuit of IHC and DAC microscopy experiments to explore the feasibility of a VEGFR-1 probe for optical molecular imaging. The low percentage of cells (~5%) that stained positively for VEGFR-1 through flow cytometry may have been due to the presence of VEGFR-1–positive endothelial cells (GFP-negative) competing for the antibody probe or removal of surface proteins by papain. However, because the experimental conditions for this initial investigation differ significantly from the intended imaging application, additional steps were not taken to optimize the initial flow cytometry screening experiments.

IHC and DAC microscopy of fresh thick tissues were performed to determine if our VEGFR-1 probe could provide adequate molecular image contrast to differentiate between tumor and normal regions in intact tissues. It should be noted that, because our probes are intended for real-time topical application during neurosurgery, we limited our staining durations to a maximum of 10 to 15 minutes to mimic the challenging time constraints of a clinical setting. Other studies have previously demonstrated a similar rapid topical application approach in the literature [22–24], with reported penetration depths as high as 1 mm [25] with significant probe binding and/or activation in as little as 1 to 5 minutes [23,24]. The fact that our VEGFR-1 probe performs well under these short incubation time constraints is a significant finding.

Results indicate that the VEGFR-1 probe is effective in differentiating between tumor and normal tissues at the margins. It is noted that while the VEGFR-1 probe exhibits a significantly higher tumor-to-normal intensity ratio than the isotype control probe ($P < .01$), the tumor-to-normal ratios are elevated for both the specific and nonspecific probes. This may be due to an enhanced permeability and retention effect that is seen in many tumors [26]. In our experience, ambiguity in image contrast during *in vivo* molecular imaging can

also be present due to nonspecific chemical binding, uneven probe distribution, and/or poor washout of unbound probes. These problems are exacerbated during *in vivo* microscopy, because the small fields of view provided by a microscope often prevent one from visualizing differential contrast between tumor and normal tissue regions within a single image frame. By using a calibrated ratiometric imaging method, we are able to distinguish between molecularly specific and nonspecific probe binding and to quantify these levels at the cellular level, thus providing an unambiguous determination of tissue status within a single image. Recently, others have shown that this technique may be used to quantify the binding potential of tumor receptors following the systemic delivery of a targeted and an untargeted imaging agent [27].

The ability to resolve individual cells with intraoperative confocal microscopy, while generally limited to a small field of view, may be of great value in cases where tumor cells are loosely distributed, such as at the margins of diffuse gliomas. In addition, certain probes, though targeted, may only label a sparse subset of tumor cells. For example, in recent years, fluorescence image–guided surgery with contrast provided by 5-aminolevulinic acid (5-ALA)–induced protoporphyrin IX fluorescence has been demonstrated to improve outcomes for patients with high-grade gliomas (World Health Organization Grades III and IV) [5,9,28]. Unfortunately, 5-ALA–induced protoporphyrin IX fluorescence is only generated in sparse proliferative cell populations and is undetectable in low-grade gliomas (World Health Organization Grades I and II) through wide-field techniques [29,30]. However, it has recently been reported that intraoperative cellular resolution confocal microscopy can be used to visualize the sparse fluorescent cells in low-grade glioma patients treated with 5-ALA [9]. Therefore, intraoperative confocal microscopy has the potential to serve as a valuable complement to wide-field techniques for the image-guided resection of certain tumors.

Future plans are to investigate the ability of the VEGFR-1 fluorescent probe, used in conjunction with a surgical DAC microscope, to enhance surgical resection in animal models. To achieve this goal, we are developing a miniature multicolor DAC microscope for *in vivo* ratiometric imaging of VEGFR-1 expression. Use of a transgenic mouse model allows for the minimization of experimental variability while optimizing these imaging technologies. However, our ultimate goal is to translate these synergistic technologies into the clinic for guiding brain tumor resection through the unambiguous real-time delineation of tumor margins in human patients.

Acknowledgments

We thank Matthew Scott from Stanford University for providing us with the transgenic mouse model. We also thank Siddhartha Mitra and James Kim from Stanford Medical School along with Adan Aguirre from the Department of Pharmacology of Stony Brook University for providing helpful insights on the primary isolation of cells from mouse cerebellum.

References

[1] Jenkin D, Greenberg M, Hoffman H, Hendrick B, Humphreys R, and Vatter A (1995). Brain tumors in children: long-term survival after radiation treatment. *Int J Radiat Oncol Biol Phys* **31**, 445–451.

[2] Nomura Y, Yasumoto S, Yanai F, Akiyoshi H, Inoue T, Nibu K, Tsugu H, Fukushima T, and Hirose S (2009). Survival and late effects on development of patients with infantile brain tumor. *Pediatr Int* **51**, 337–341.

[3] Albright AL, Wisoff JH, Zeltzer PM, Boyett JM, Rorke LB, and Stanley P (1996). Effects of medulloblastoma resections on outcome in children: a report from the Children's Cancer Group. *Neurosurgery* **38**, 265–271.

[4] Liu JT, Mandella MJ, Loewke NO, Haeberle H, Ra H, Piyawattanametha W, Solgaard O, Kino GS, and Contag CH (2010). Micromirror-scanned dual-axis confocal microscope utilizing a gradient-index relay lens for image guidance during brain surgery. *J Biomed Opt* **15**, 026029.

[5] Stummer W, Pichlmeier U, Meinel T, Wiestler OD, Zanella F, and Reulen HJ (2006). Fluorescence-guided surgery with 5-aminolevulinic acid for resection of malignant glioma: a randomised controlled multicentre phase III trial. *Lancet Oncol* **7**, 392–401.

[6] van Dam GM, Themelis G, Crane LM, Harlaar NJ, Pleijhuis RG, Kelder W, Sarantopoulos A, de Jong JS, Arts HJ, van der Zee AG, et al. (2011). Intraoperative tumor-specific fluorescence imaging in ovarian cancer by folate receptor-α targeting: first in-human results. *Nat Med* **17**, 1315–1319.

[7] Nguyen QT, Olson ES, Aguilera TA, Jiang T, Scadeng M, Ellies LG, and Tsien RY (2010). Surgery with molecular fluorescence imaging using activatable cell-penetrating peptides decreases residual cancer and improves survival. *Proc Natl Acad Sci USA* **107**, 4317–4322.

[8] Sanai N, Polley MY, McDermott MW, Parsa AT, and Berger MS (2011). An extent of resection threshold for newly diagnosed glioblastomas. *J Neurosurg* **115**, 3–8.

[9] Sanai N, Snyder LA, Honea NJ, Coons SW, Eschbacher JM, Smith KA, and Spetzler RF (2011). Intraoperative confocal microscopy in the visualization of 5-aminolevulinic acid fluorescence in low-grade gliomas. *J Neurosurg* **115**, 740–748.

[10] Schlosser HG, Suess O, Vajkoczy P, van Landeghem FK, Zeitz M, and Bojarski C (2010). Confocal neurolasermicroscopy in human brain—perspectives for neurosurgery on a cellular level (including additional comments to this article). *Cent Eur Neurosurg* **71**, 13–19.

[11] Sankar T, Delaney PM, Ryan RW, Eschbacher J, Abdelwahab M, Nakaji P, Coons SW, Scheck AC, Smith KA, Spetzler RF, et al. (2010). Miniaturized handheld confocal microscopy for neurosurgery: results in an experimental glioblastoma model. *Neurosurgery* **66**, 410–417; discussion 417–418.

[12] Slongo ML, Molena B, Brunati AM, Frasson M, Gardiman M, Carli M, Perilongo G, Rosolen A, and Onisto M (2007). Functional VEGF and VEGF receptors are expressed in human medulloblastomas. *Neuro Oncol* **9**, 384–392.

[13] Goodrich LV, Milenkovic L, Higgins KM, and Scott MP (1997). Altered neural cell fates and medulloblastoma in mouse patched mutants. *Science* **277**, 1109–1113.

[14] Wetmore C, Eberhart DE, and Curran T (2001). Loss of p53 but not ARF accelerates medulloblastoma in mice heterozygous for patched. *Cancer Res* **61**, 513–516.

[15] Liu JT, Mandella MJ, Crawford JM, Contag CH, Wang TD, and Kino GS (2008). Efficient rejection of scattered light enables deep optical sectioning in turbid media with low-numerical-aperture optics in a dual-axis confocal architecture. *J Biomed Opt* **13**, 034020.

[16] Liu JT, Helms MW, Mandella MJ, Crawford JM, Kino GS, and Contag CH (2009). Quantifying cell-surface biomarker expression in thick tissues with ratiometric three-dimensional microscopy. *Biophys J* **96**, 2405–2414.

[17] Liu JT, Mandella MJ, Friedland S, Soetikno R, Crawford JM, Contag CH, Kino GS, and Wang TD (2006). Dual-axes confocal reflectance microscope for distinguishing colonic neoplasia. *J Biomed Opt* **11**, 054019.

[18] Brewer GJ and Torricelli JR (2007). Isolation and culture of adult neurons and neurospheres. *Nat Protoc* **2**, 1490–1498.

[19] Abramoff MD, Magalhaes PJ, and Ram SJ (2004). Image processing with ImageJ. *Biophotonics Int* **11**, 36–42.

[20] De Rosa FS, Marchetti JM, Thomazini JA, Tedesco AC, and Bentley MV (2000). A vehicle for photodynamic therapy of skin cancer: influence of dimethylsulphoxide on 5-aminolevulinic acid *in vitro* cutaneous permeation and *in vivo* protoporphyrin IX accumulation determined by confocal microscopy. *J Control Release* **65**, 359–366.

[21] Kurihara-Bergstrom T, Flynn GL, and Higuchi WI (1987). Physicochemical study of percutaneous absorption enhancement by dimethyl sulfoxide: dimethyl sulfoxide mediation of vidarabine (ara-A) permeation of hairless mouse skin. *J Invest Dermatol* **89**, 274–280.

[22] Nitin N, Rosbach KJ, El-Naggar A, Williams M, Gillenwater A, and Richards-Kortum RR (2009). Optical molecular imaging of epidermal growth factor receptor expression to improve detection of oral neoplasia. *Neoplasia* **11**, 542–551.

[23] Cutter JL, Cohen NT, Wang J, Sloan AE, Cohen AR, Panneerselvam A, Schluchter M, Blum G, Bogyo M, and Basilion JP (2012). Topical application of activity-based probes for visualization of brain tumor tissue. *PLoS One* **7**, e33060.

[24] Urano Y, Sakabe M, Kosaka N, Ogawa M, Mitsunaga M, Asanuma D, Kamiya M, Young MR, Nagano T, Choyke PL, et al. (2011). Rapid cancer detection by topically spraying a γ-glutamyltranspeptidase–activated fluorescent probe. *Sci Transl Med* **3**, 110ra119.

[25] Leunig A, Mehlmann M, Betz C, Stepp H, Arbogast S, Grevers G, and Baumgartner R (2001). Fluorescence staining of oral cancer using a topical application of 5-aminolevulinic acid: fluorescence microscopic studies. *J Photochem Photobiol B* **60**, 44–49.

[26] Matsumura Y and Maeda H (1986). A new concept for macromolecular therapeutics in cancer chemotherapy: mechanism of tumoritropic accumulation of proteins and the antitumor agent smancs. *Cancer Res* **46**, 6387–6392.

[27] Tichauer KM, Samkoe KS, Sexton KJ, Hextrum SK, Yang HH, Klubben WS, Gunn JR, Hasan T, and Pogue BW (2011). *In vivo* quantification of tumor receptor binding potential with dual-reporter molecular imaging. *Mol Imaging Biol* **14**, 584–592.

[28] Nabavi A, Thurm H, Zountsas B, Pietsch T, Lanfermann H, Pichlmeier U, and Mehdorn M (2009). Five-aminolevulinic acid for fluorescence-guided resection of recurrent malignant gliomas: a phase II study. *Neurosurgery* **65**, 1070–1076; discussion 1076–1077.

[29] Ishihara R (2007). Quantitative spectroscopic analysis of 5-aminolevulinic acid-induced protoporphyrin IX fluorescence intensity in diffusely infiltrating astrocytomas. *Neurol Med Chir (Tokyo)* **47**, 53–57.

[30] Widhalm G, Wolfsberger S, Minchev G, Woehrer A, Krssak M, Czech T, Prayer D, Asenbaum S, Hainfellner JA, and Knosp E (2010). 5-Aminolevulinic acid is a promising marker for detection of anaplastic foci in diffusely infiltrating gliomas with nonsignificant contrast enhancement. *Cancer* **116**, 1545–1552.